RSC Advances

This article can be cited before page numbers have been issued, to do this please use: R. Kundu and C. Kulshreshtha, *RSC Adv.*, 2015, DOI: 10.1039/C5RA13416A.

View Article Online
DOI: 10.1039/C5RA13416A

Design, synthesis and electronic properties of push-pull-push type dye

Rajen Kundu,*[a] Chandramouli Kulshreshtha *[b]

[a] Department of Chemistry, Pohang University of Science and Technology, Pohang 790-784, Republic of Korea
[b] Department of Chemical Engineering, Pohang University of Science and Technology, Pohang 790-784, Republic of Korea

Graphical abstract

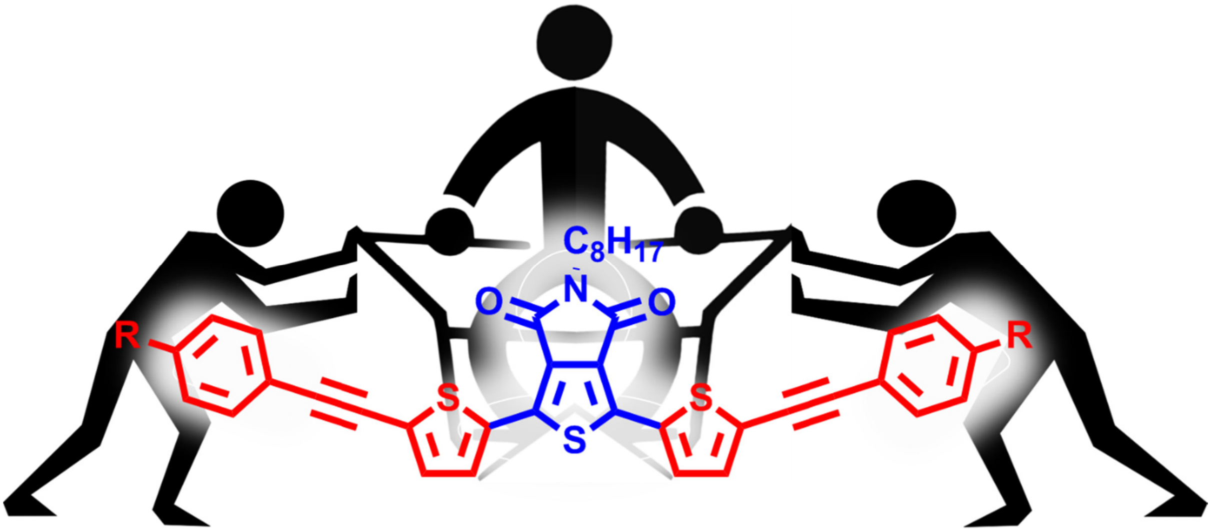

View Article Online
DOI: 10.1039/C5RA13416A

Journal Name

ARTICLE

Design, synthesis and electronic properties of push-pull-push type dye

Received 00th January 20xx,
Accepted 00th January 20xx

DOI: 10.1039/x0xx00000x

www.rsc.org/

Rajen Kundu,*[a] Chandramouli Kulshreshtha *[b]

Sonogashira cross-coupling protocol was employed for the construction of a push-pull-push type dye. Ethynyl π-spacer extends the effective π-conjugation length between push and pull units without altering the planarity of the electron donor/acceptor pair. The variation of the strength of alkyne π-spacer electron push (or donor) units of these dyes has a strong effect towards the shifting of both absorption and emission maxima and thereby on the Stokes shift. The dyes we solvatochromic and their solvatochromicity was highly dependent on the electron push unit. Strong red shifted emissic were likely to arise due to the internal charge transfer (ICT) from electron push unit to electron pull unit. Calculated energy values of HOMO→LUMO transitions are in good accordance with experimental observations. Alkyne conjugated electron push units (–C≡C–Ar; Ar = Ph, Ph-OMe, Ph-NMe$_2$) are more effective to increase the E_{HOMO} levels. Overall, experimental and theoretical results of the push-pull-push dyes indicate that they can be used as a promising conjugated materials with predictable electronic properties for optoelectronic devices.

Introduction

π-Conjugated donor-acceptor type molecules have been widely used in material science as an efficient organic electronics material for applications in organic light-emitting diode (OLED), [1-5] organic field effect transistor (OFET), [6-13] organic photovoltaic device (OPV) [14-29] and so forth. Ethynyl (–C≡C–) and vinyl (–HC=CH–) π-conjugates are structurally very similar and could potentially reduce the band gap energy. [30-35] However, vinyl π-conjugated systems show better charge delocalization and smaller band gap energy over the ethynyl π-conjugation. [36] Indeed, an ethynyl π-spacer is sterically less hindered and more accommodating than a vinyl π-spacer. [37] It is also noteworthy that the steric crowd between face-to-face groups of vinyl and aromatic units result a non-planar conformation, which reduces the charge delocalization efficiency. [38-39] Additionally, the incorporation of an ethynyl π-spacer is a straightforward approach and easier than a vinyl π-spacer in synthetic point of view. [40-41] Thus, design and synthesis of novel ethynyl π-conjugated donor-acceptor type molecules having high performance material properties remain a promising area of optoelectronic research. The push-pull-push type dye structure, where the electron donating units push the negative charge density and electron accepting units pull the negative charge density towards itself. Both the push and pull units are connected by π-conjugated alkyne (–C≡C–) spacer unit which enables the intramolecular charge transfer (ICT) from electron rich (push) to electron deficient (pull) units, and thereby facilitates red shifted absorbance with high molar extinction coefficient. [42-51] The electron deficient unit tunes the energy levels of frontier molecular orbitals and at the same time the π-conjugated alkyne spacer connected electron rich unit also involves to monitor the energy levels. [17] According to the donor capability of the donating unit, we can monitor the energy level of the highest occupied molecular orbita (HOMO) and lowest unoccupied molecular orbital (LUMO) and can obtain different physical properties. [17, 52-59]

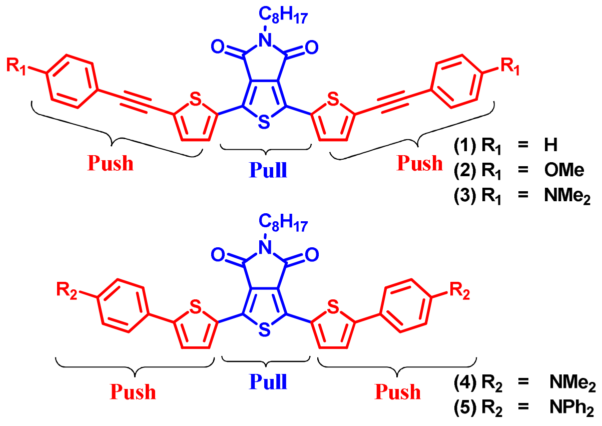

Fig. 1 Chemical structures of push-pull-push dye.

In our study, we demonstrate the incorporation of an alkyne π-spacer between the donor (push) and acceptor (pull) units. T alkyne π-spacer was introduced to extend the effective conjugatio

---

[a] Department of Chemistry, Pohang University of Science and Technology, Pohang 790-784, Republic of Korea. Email: kundurajen@postech.ac.kr

[b] Department of Chemical Engineering, Pohang University of Science and Technology, Pohang 790-784, Republic of Korea. Email: mouli@postech.ac.kr

† Electronic Supplementary Information (ESI) available: Normalized UV-visible and fluorescence spectra, fluorescence images of the dyes, cyclic voltammograms, cartesian coordinates, NMR spectra. See DOI: 10.1039/x0xx00000x

and improve the photophysical properties. [31, 60-61] In addition, the planer structure of alkyne facilitates efficient charge transport which can improve the optoelectronic properties. We chose the readily synthesizable thieno-[3,4-c]pyrrole-4,6-dione (TPD) as an electron pull unit which is symmetric, rigidly fused planer structure having strong electron withdrawing property. [62-72] This unit provides low energy HOMO level, low band gap, and is convenient for the introduction of variety of alkyl side chains into the pyrrole ring to improve the solubility in organic solvents. Varieties of ethynyl donar groups (Ar–C≡C–) are commercially available or easily synthesizable according to the requirement. Sonogashira cross-coupling gives the facile synthetic advantage of structural variation in the electron push unit of the push-pull-push dye. Overall, the dyes showed tunable electronic properties. Herein, we investigated the effect on variation of the strength of alkyne π-spacer electron donor units of the push-pull-push dye using a combination of experimental and theoretical studies.

Results and discussion

Synthesis

The push-pull-push dyes were synthesized by cross coupling reaction between the donor (push) and acceptor (pull) units and are shown in Scheme 1. Sonogashira coupling [40-41] was used to synthesize alkyne π-spacer conjugated dyes and Suzuki coupling [73] was used to attach the donor and acceptor units directly via C(sp2)–C(sp2) coupling without alkyne π-spacer. The TPD acceptor unit was synthesized from thiophene-3,4-dicarboxylic acid. [62-64] Thus, the refluxing of thiophene-3,4-dicarboxylic acid (**6**) in acetic anhydride gave thiophene-3,4-dicarboxylic anhydride (**7**), which when treated with n-octylamine followed by stirring with thionyl chloride afforded the TPD unit, 5-octyl-4H-thieno[3,4-c]pyrrole-4,6(5H)-dione (**9**). Compound **9** was brominated to give dibromo product (**10**), which was further reacted with 2-(tributylstannyl)thiophene to yield 5-octyl-1,3-di(thiophen-2-yl)-4H-thieno[3,4-c]pyrrole-4,6(5H)-dione (**11**). Bromination of **11** using *N*-bromosuccinimide and prolonged reaction time resulted in symmetric dibromo compound **12**. Finally, the dyes **1**–**3** were synthesized via C(sp2)–C(sp3) Sonogashira coupling between **12** and terminal alkynes **13**–**15**. Whereas the dyes **4**–**5** were synthesized via C(sp2)–C(sp2) Suzuki coupling between **12** and boronic acids **16**–**17**. The intermediate and final products were characterized by NMR and ESI MS (see ESI†). The very pure and recrystallized form of the dyes (**1**–**5**) were used to study the photophysical and optoelectronic properties.

Photophysical properties

First, we investigated the absorption photophysical properties of the dyes (**1**–**5**) in different solvents of varying dielectric constants. We observed 10 to 20 nm bathochromic shift of all the dyes upon changing the solvent polarity from nonpolar hexane to polar solvent dimethyl sulfoxide (DMSO). However, in polar protic solvent MeOH, we observed hypsochromic shift, and this is because of protic solvent–solute interaction between the dye and the solvent.[74-75]

View Article Online
DOI: 10.1039/C5RA13416A

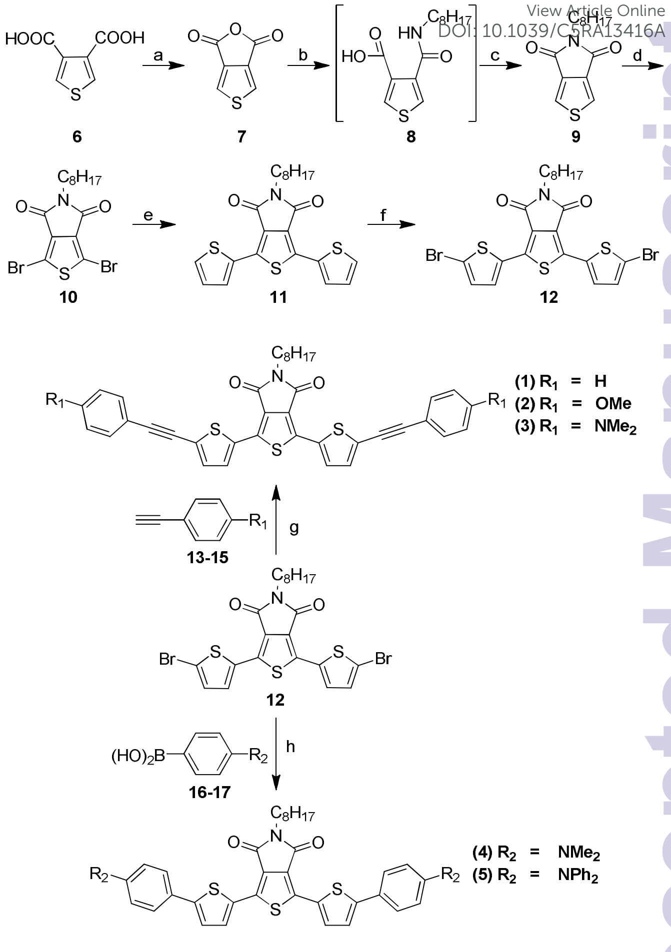

Scheme 1 Synthesis of push-pull-push dye **1**–**5**. Reagents and conditions: (a) $(CH_3CO)_2O$, heat 140 °C, 12h; (b) $C_8H_{17}NH_2$, toluene, reflux, 24h; (c) $SOCl_2$, 5 °C, 8h; (d) *N*-bromosuccinimide (NBS), H_2SO_4, CF_3COOH, 10h; (e) 2-(tributylstannyl)thiophene, $Pd_2(dba)_2$, tri(O-tolyl)phosphine, toluene, reflux, 18h; (f) NBS, $CHCl_3$, CH_3COOH, 0 °C to rt, 30h; (g) $Pd(PPh_3)_4$, CuI, N,N-diisopropylethylamine (DIPEA), DMF, 80 °C, 24h; (h) $Pd(PPh_3)_2Cl_2$, K_3PO_4, DMF, 80 °C, 24h.

Inconsistency behaviour in the absorption maxima was shown in some of the intermediate polar solvents. Donating groups have a strong effect on monitoring the absorptive properties of the dyes **1**–**3**. The dye **1** containing phenyl group as the electron push unit shows average absorption maxima at around 440 nm and lies between 433 – 440 nm; whereas, dye **3** containing 4-N,N-dimethylaniline group as electron push unit showed absorption maxima at around 470 nm and lies between 465 – 485 nm (Fig. 2 a, e). The intermediate electron push unit 4-methoxyphenyl shows absorption maxima at around 450 nm and lies between 446 – 456 nm (Fig. 2 c). Thus, we observed ~10 nm bathochromic shift from the dye **1** to **2**, by changing the electron push unit phenyl (–Ph–H) to 4-methoxyphenyl (–Ph–OMe) group and ~30 nm bathochromic shift from the dye **1** to **3**, by changing phenyl (–Ph–H) to more efficient electron push unit 4-N,N-dimethylaniline (–Ph–NMe_2) group. The dyes **4** and **5** absorb between 468 – 488 nm. However, the molar extinction

View Article Online
DOI: 10.1039/C5RA13416A

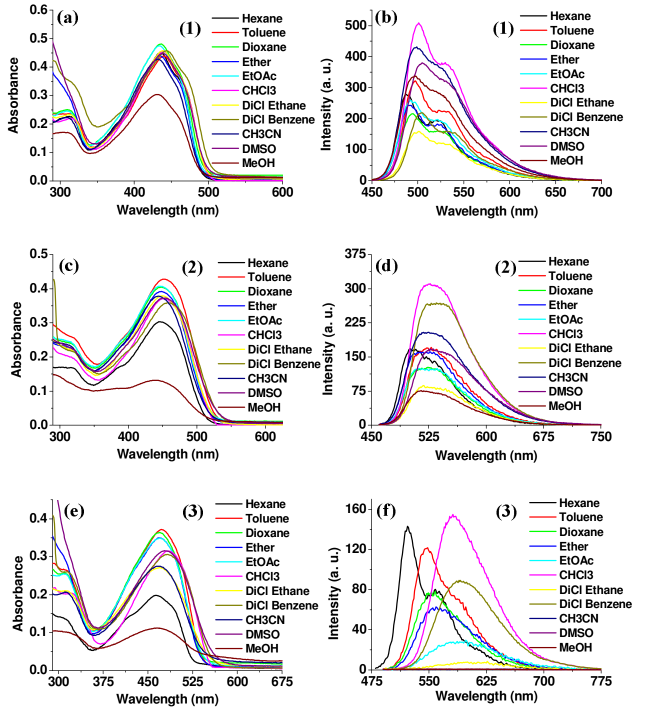

Fig. 2 UV-visible (a, c, e) and fluorescence (b, d, f) spectra of the dyes **1**, **2** and **3** respectively in different solvents (10 µM, RT, $\lambda_{ex} = \lambda_{UV\ max}$ of each solvents). Inset: Normalized UV- visible spectra of each dye.

coefficient of the dye **5** is more and almost doubled compared to the dye **4** and this is because –NPh$_2$ group in dye **5** provides larger conjugated system than –NMe$_2$ group provides in dye **4** (Fig. 3 a, c).

Next, we evaluated the fluorescence emission behaviour of the dyes (**1**–**5**) in different solvents moving from nonpolar hexane to polar MeOH solvents (Fig. 2 b, d, f and Fig. 3 b, d). We observed very interesting solvent dependent emission properties upon changing the electron push unit. The emission properties of the dyes were more effective on solvent polarity than the absorption properties. All the dyes showed structured band in low polar or medium polar solvents and structureless broad emission band in high polar solvents. Interestingly, for all the cases we observed strong red shifted fluorescence emission with decrease in fluorescence intensity as the solvent polarity changes from nonpolar to polar. These results clearly indicate that the emission bands were arise due to the internal charge transfer (ICT) from electron push unit to electron pull unit. The large Stokes shift was observed with increasing solvent polarity of all the dyes and it was also highly affected by the electron push unit and the π-conjugation (Table 1, and see ESI†). The electron donor units used in this study follow the order –Ph–H < –Ph–OMe < –Ph–NPh$_2$ ≤ –Ph–NMe$_2$. With increasing solvent polarity a red shift of about 20 nm ($\lambda_{max,Hexane}$ = 487 nm and $\lambda_{max,DMSO}$ = 507 nm) for the dye **1** (containing phenyl (–Ph–H) as electron push unit) was observed. Replacement of the phenyl (–Ph–H) group in dye **1** with a strong electron donating 4-N,N-dimethylaniline (–Ph–NMe$_2$) group in dye **3** leads to a strong red shift of about 75 nm ($\lambda_{max,Hexane}$ = 520 nm and $\lambda_{max,EtOAc}$ = 595 nm). The moderate electron donating group 4-methoxyphenyl (–Ph–OMe) containing dye **2** showed 40 nm red shift from hexane ($\lambda_{max,Hexane}$ = 500 nm) to dichlorobenzene ($\lambda_{max,Dichlorobenzene}$ = 540 nm) (see ESI†). As –Ph–NMe$_2$ group is the strongest electron donating group among the four, so best charge delocalization through the alkyne π-spacer occurs in dye **3** and it shows highest absorption and emission maxima and also lowest band gap energy. Thus, from the above observations it is clear that the electron push units of these push-pull-push dyes have a strong effect towards the shifting of both absorption and emission maxima and thereby on the Stokes shift. The lack of alkyne π-spacer conjugation reduces the red shift to 45 nm ($\lambda_{max,Hexane}$ = 533 nm and $\lambda_{max,EtOAc}$ = 578 nm) in dye **4** although it contains the strong electron donating 4-N,N-dimethylaniline (–Ph–NMe$_2$) group. Dye **5** containing the electron push unit 4-N,N-diphenylaniline (–Ph–NPh$_2$) group showed 85 nm ($\lambda_{max,Hexane}$ = 530 nm and $\lambda_{max,DMSO}$ = 615 nm) red shift although it does not contain the alkyne π-spacer conjugation. The large conjugated system due to the –NPh$_2$ group compensates the lack of alkyne π-spacer conjugation and leads to a strong red shifted emission. Both the fluorescence intensity and the quantum yield were decreased with increasing solvent polarity for all the dyes (**1**–**5**). All the above observations revealed that the dyes were solvatochromic and their solvatochromicity was highly dependent on the electron push unit and the π- conjugation. The photophysical properties of the dyes (**1**–**5**) in CHCl$_3$ solutions are summarized in Table 1.

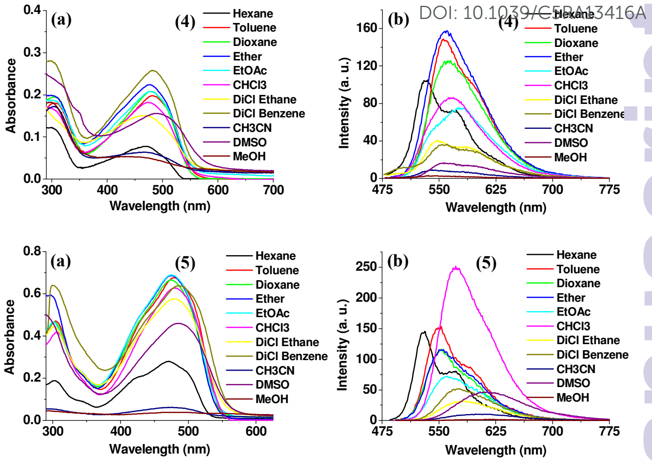

Fig. 3 UV-visible (a, c) and fluorescence (b, d) spectra of the dyes **4** and **5** respectively in different solvents (10 µM, RT, $\lambda_{ex} = \lambda_{UV\ max}$ of each solvents). Inset: Normalized UV- visible spectra of each dye.

The solvatochromicity of the dyes (**1**–**5**) was reflected on the colour of the fluorescence images, which changed in different solvents under a 254 nm wavelength transilluminator (see ESI†). The influence of electron donating units on the shifting of emission maxima of these push-pull-push dyes was also nicely observed by the colour change in chloroform solvent under a

View Article Online
DOI: 10.1039/C5RA13416A

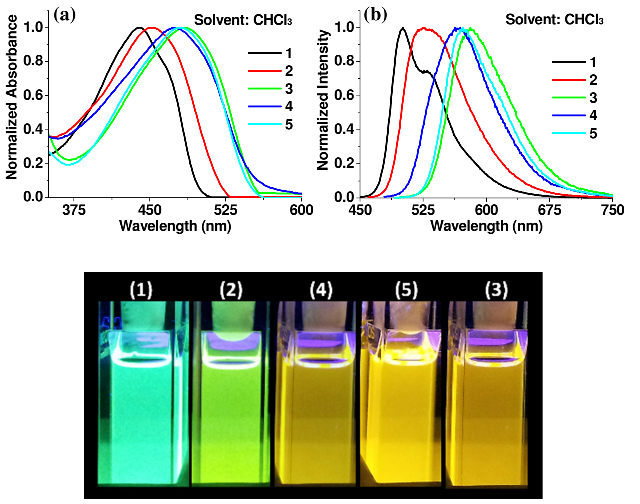

Fig. 4 Normalized (a) UV-visible and (b) fluorescence spectra the dyes **1–5** in $CHCl_3$ solvents (10 µM, RT, $\lambda_{ex} = \lambda_{UV\,max}$). (c) Colours: colours in $CHCl_3$ solvents after irradiation of **1–5** in UV light (λ = 254 nm) under a UV-transilluminator.

Table 1. Photophysical properties[a] of the dye **1–5**

Dye	$\lambda_{max(Abs)}$ (nm)	ε_{max} $M^{-1}cm^{-1}$	$\lambda_{max(Em)}$ (nm)	Stokes shift (cm^{-1})	Φ_F[b]
1	440	45400	501	2767	0.119
2	453	37100	529	3171	0.142
3	485	30600	581	3406	0.096
4	477	18000	566	3296	0.096
5	482	62500	572	3264	0.071

[a] Photophysical data in $CHCl_3$ solvent. [b] Quantum yield using fluorescein in 0.1 N NaOH as a standard ($\Phi_f = 0.92$), $\lambda_{ex} = 440, 453, 480$ nm

254 nm wavelength transilluminator (Fig. 4). The colour varies from cyan to green to yellow to orange region accordingly with the electron donating capacity (–Ph–H < –Ph–OMe < –Ph–NPh₂ ≤ –Ph–NMe₂) of the electron push unit and the extra π-conjugation effect.

After solution state photophysical study, we investigated the solid state photophysical properties of the dyes (**1**–**5**) as film. To measure thin films, dyes were spin coated on pre-cleaned quartz substrates using chloroform solutions. To ensure the smooth films, spin coating time and speed were fixed at 60s and 1000 rpm. It is noteworthy that both the solution and solid state results follow similar trends. The UV-visible absorption and fluorescence spectra of the dyes (**1**–**5**) in the film state are shown in Fig. 5. The dyes **1**–**5** exhibit absorption peak centered at 456, 456, 494, 480, and 485 nm respectively. Thus, all the synthesized push-pull-push dyes (**1**–**5**) absorbs visible light. The fluorescence emission maxima of the dyes **1**–**5** centered at 583, 610, 652, 623, and 638 nm respectively. Dye **3** showed highest absorption and emission maxima among all the dyes **1**–**5**, which can be attributed to increase in strength of the electron donating group and π-conjugation. Thus, the effect of electron donating groups and the of alkyne π-spacer conjugation also reflected on the photophysical properties in film state.

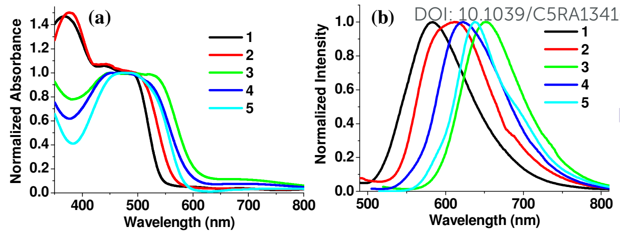

Fig. 5 Normalized (a) UV-visible and (b) fluorescence spectra of the dyes **1–5** as film, spin coated on pre-cleaned quartz substrates using chloroform solutions.

Computational studies

Highest occupied molecular orbitals (HOMO) and lowest unoccupied molecular orbitals (LUMO) of push-pull-push dye (**1**–**5**) have been calculated using Gaussian 03 program package.[76] First the geometries were optimized using the B3LYP hybrid density functional and 3-21G* as the basis set. Next, the optimized geometries were used for TD-SCF calculation using the same B3LYP hybrid density functional and 3-21G* as the basis set. For all the dyes, HOMO resides mainly on the electron push units and/or alkyne π-spacer including thiophene units. In contrast, LUMO resides mainly on the TPD moiety and delocalized nearby two thiophene units attached with TPD moiety. The electron density diagrams of HOMO and LUMO are shown in Fig. 6. The calculated allowed transitions are listed in Table 2. The lowest energy associated with strong absorption band arises from $S_0 \rightarrow S_1$ transition which is attributed to the electronic transition from HOMO→LUMO.

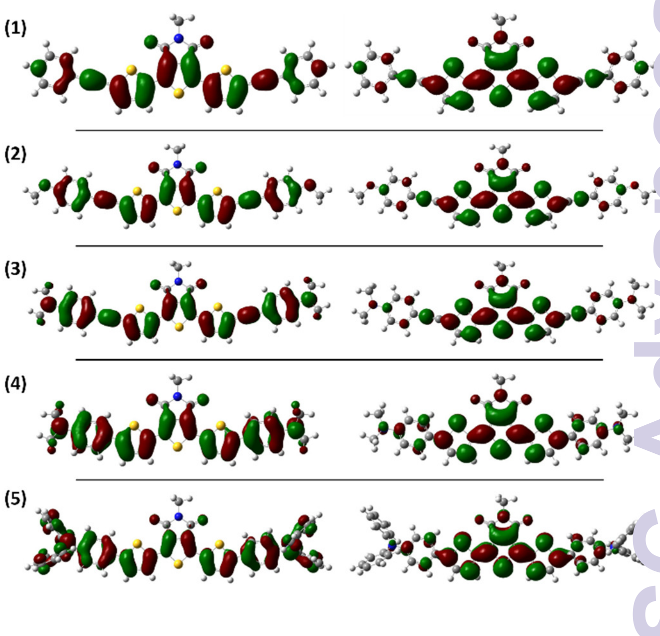

Fig. 6 HOMOs (left) and LUMOs (right) of push-pull-push dye (**1–5**) (calculated using Gaussian 03; Opt+Freq: B3LYP/3-21G* // TD-SCF: B3LYP/3-21G*).

View Article Online
DOI: 10.1039/C5RA13416A

Table **2**. Calculated lowest energy $S_0 \rightarrow S_1$ transition

Dye	Electronic transition	Wavelength (nm)	Oscillator strengths	Major contributions HOMO→LUMO
1	$S_0 \rightarrow S_1$	485	1.8147	83.9%
2	$S_0 \rightarrow S_1$	505	1.9778	85.0%
3	$S_0 \rightarrow S_1$	546	2.0238	86.9%
4	$S_0 \rightarrow S_1$	510	1.5026	86.5%
5	$S_0 \rightarrow S_1$	528	1.6926	88.8%

Thus, all these low energy strong absorptions mostly (84% to 89%) originated from HOMO→LUMO correspond to $\pi \rightarrow \pi^*$ transitions which arise due to intramolecular charge transfer (ICT) from electron push units to electron pull TPD unit through the π-conjugation. The calculated energy values for $S_0 \rightarrow S_1$ transition of the dye **1**–**5** were in good agreement with the experimental absorption energy values (Table 1–2).

Cyclic voltammetry studies

To evaluate the energy parameters of the dye **1**–**5**, cyclic voltammetry (CV) measurements were carried out. Ferrocene/ferrocenium (Fc/Fc^+) redox couple was used as an internal reference. The HOMO and LUMO energy levels were calculated from the onset of the first oxidation and reduction potentials using the equations E_{HOMO} (eV) = - [$E_{\mathrm{ox}}^{\mathrm{onset}}$ - $E_{1/2}$ (Fc/Fc^+) + 4.8] and E_{LUMO} (eV) = - [$E_{\mathrm{red}}^{\mathrm{onset}}$ - $E_{1/2}$ (Fc/Fc^+) + 4.8], where $E_{1/2}$ (Fc/Fc^+) was the cell correction. It showed two peaks at 0.389 and 0.485 V hence the $E_{1/2}$ (Fc/Fc^+) was equal to 0.437 V, which was used in equation to calculate the E_{HOMO} and E_{LUMO}. The energy parameters of the dye (**1**–**5**) are summarized in Table 3 (see ESI† for the cyclic voltammogram). Thus, the summarized E_{HOMO} and E_{LUMO} values show that the alkyne conjugated electron push unit (–C≡C–Ar; Ar = Ph, Ph-OMe, Ph-NMe_2) is more effective to increase the E_{HOMO} levels. However, the E_{LUMO} levels are not significantly affected by the electron push unit. It is noteworthy that band gap energy decreases upon introducing electron donor units into **11**. The decrease in E_{LUMO} and increase in E_{HOMO} levels of the dyes (**1**–**5**) upon introducing electron donor units into **11** can be explained in terms of inductive effect and resonance effect.[17] TPD is a strong electron withdrawing unit and shows strong inductive effect. The conjugated electron donor units show resonance effect and able to delocalize the charge density and or π-system with neighbouring ethynyl π-spacer and or thiophene unit. Thus, both the inductive effect and resonance effect increases the effective delocalization which strongly affect the E_{HOMO} and E_{LUMO} levels to reduce the band gap energy of the dyes (**1**–**5**).

Table 3. Energy parameters of the dye **1**–**5**

Dye	E_{ox} (V)	E_{red} (V)	E_{HOMO} (eV)	E_{LUMO} (eV)	$E_{\mathrm{ox\text{-}red}}$ (eV)
1	1.28	-0.754	-5.643	-3.609	2.034
2	1.11	-0.689	-5.473	-3.674	1.799
3	0.826	-0.76	-5.189	-3.603	1.586
4	0.856	-0.73	-5.219	-3.633	1.586
5	0.566	-0.853	-4.929	-3.51	1.419

Overall, the electron donor units of these push-pull-push dye carefully balance both the E_{HOMO} and E_{LUMO} levels, which make them promising optoelectronics material.

Conclusions

In summary, we have synthesized push-pull-push type dyes and investigated the electronic properties using a combination of both experimental and theoretical studies. Ethynyl π-spacer improved the electronic properties of the dye by extending the effective π-conjugation between electron donor/acceptor units. All the dyes showed highly solvent dependent red shifted emission and large Stokes shift. The solvatochromism of the dyes significantly depends on the strength of the electron donor unit. The red shifted emissions were assigned as internal charge transfer (ICT) between electron donor/acceptor pair. The influence of electron donating units on the shifting of emission maxima of these push-pull-push dyes were reflected on the colour change in chloroform solvent under a 254 nm wavelength transilluminator. Strong electron donating 4-N,N-dimethylaniline (–Ph–NMe_2) group in dye **3** leads to a strong red shift of about 75 nm ($\lambda_{\mathrm{max,Hexane}}$ = 520 nm and $\lambda_{\mathrm{max,EtOAc}}$ = 595 nm). Calculated energy values of HOMO→LUMO transitions are in good agreement with experimental observations. The electron push units (–C≡C–Ar; Ar = Ph, Ph-OMe, Ph-NMe_2) are more effective to increase the E_{HOMO} levels. However, the E_{LUMO} levels are not significantly affected by the electron push unit. Overall, findings indicate that these push-pull-push dyes can be used as a promising conjugated materials with predictable electronic properties for optoelectronic devices.

Experimental section

General

All the reagents and solvents were purchased from commercial suppliers and were used without further purification. The air- and/or moisture-sensitive reactions were carried out under nitrogen atmosphere. All the reactions were monitored with analytical TLC silica gel 60 F_{254}. The products were purified by silica gel (230-400 mesh size) column chromatography. ^1H and ^{13}C NMR spectra were recorded under 400 MHz and 100 MHz Bruker Advance NMR spectrometer respectively using $CDCl_3$ as the solvent. All the UV–visible spectra of the compounds (10 μM) were measured in different solvents using a UV-Visible spectrophotometer at room temp with a cell of 1 cm path length. All the sample solutions prepared for UV–visible experiments were further used for fluorescence experiments immediately after UV–visible experiments. The fluorescence spectra were obtained using a fluorescence spectrophotometer at room temp using 1 cm path length cell. The fluorescence quantum yields (Φ_f) were determined using fluorescein as a reference with the known Φ_f (0.92) in 0.1 molar solution in sodium hydroxide. The electrochemical cyclic voltammetry (CV) was conducted on a PowerLab/AD instrument model system with glassy carbon disk, Pt wire, and Ag/Ag^+ electrode as the working electrode, counter electrode, and reference electrode respectively in a 0.1 M tetrabutylammonium hexafluorophosphate (n-Bu_4NPF_6)-anhydrous acetonitrile solution at a potential scan rate of 50 mV s^{-1}. Material film was drop cast onto the glassy carbon working electrode from a 2.0 mg mL^{-1} chloroform solution and dried. The electrochemical onsets were determined at the position where the current starts to differ from the baseline. The potential of Ag/AgCl reference electrode was internally calibrated by using the ferrocene/ferrocenium redox couple (Fc/Fc^+). The HOMO and LUMO energy levels were calculated from the onset of the first oxidation and reduction potentials using the equations E_{HOMO} (eV) = - [E_{ox}^{onset} - $E_{1/2}$ (Fc/Fc^+) + 4.8] and E_{LUMO} (eV) = - [E_{red}^{onset} - $E_{1/2}$ (Fc/Fc^+) + 4.8], where $E_{1/2}$ (Fc/Fc^+) was the cell correction. Gaussian 03 program package was used for the computational study. The geometries were optimized using the B3LYP hybrid density functional and 3-21G* as the basis set. Next, the optimized geometries were used for TD-SCF calculation using the same B3LYP hybrid density functional and 3-21G* as the basis set. For all the cases imaginary frequency values after opt-freq (optimization followed by frequency) calculation were zero.

Thieno[3,4-c]furan-1,3-dione (7). A solution of 4 g (23.242 mmol) thiophene-3,4-dicarboxylic acid (**6**) in 150 mL acetic anhydride was refluxed for 12h. After the completion of reaction, the solution was evaporated under reduced pressure and the solid residue was recrystallized from hot toluene, 3.402 g, 95% yield. ^1H NMR (400 MHz, $CDCl_3$) δ 8.10 (2H, s); ^{13}C NMR (100 MHz, $CDCl_3$) δ 129.5, 135.3, 156.5; HRMS calcd for $C_6H_2O_3S$ 153.9725, found 153.9711.

5-Octyl-4H-thieno[3,4-c]pyrrole-4,6(5H)-dione (9). To a solution of 3.35 g (21.739 mmol) thieno[3,4-c]furan-1,3-dione (**7**) in toluene, 7.2 mL *n*-octylamine was added and refluxed for 24h. The reaction mixture was cooled down and the solvent was evaporated under reduced pressure. The crude solid was dissolved in 200 mL thionyl chloide ($SOCl_2$) and stirred for 8h under 50 °C. The volatile solvent was removed and the crude product was purified by silica gel (230-400 mesh size) column chromatography using hexane-dichloromethane as eluent to afford the white solid product, 3.75 g, 65% yield. ^1H NMR (400 MHz, $CDCl_3$) δ 0.87 (3H, t, *J* = 5.2 Hz), 1.25 – 1.31 (10H, m), 1.61 – 1.67 (2H, m), 3.60 (2H, t, *J* = 7.2 Hz), 7.79 (2H, s); ^{13}C NMR (100 MHz, $CDCl_3$) δ 14.2, 22.7, 27.0, 28.6, 29.2, 31.9, 38.6, 125.5, 136.8, 162.7; HRMS calcd for $C_{14}H_{19}NO_2S$ 265.1136, found 265.1125.

1,3-Dibromo-5-octyl-4H-thieno[3,4-c]pyrrole-4,6(5H)-dione (10). To a solution of 3.7 g (13.946 mmol) 5-octyl-4H-thieno[3,4-c]pyrrole-4,6(5H)-dione (**9**) in a mixture of sulfuric acid (10 mL) and trifluoroacetic acid (30 mL), 5.46 g (30.681 mmol) *N*-bromosuccinimide was added in eight portions. The reaction mixture was stirred at room temperature for 10h. The reddish brown solution was diluted with water (120 mL) and the mixture was extracted with dichloromethane. The organic layer was dried over anhydrous magnesium sulfate followed by concentrated under reduced pressure. The crude product was purified by silica gel (230-400 mesh size) column chromatography using hexane-dichloromethane as eluent to afford the white crystalline solid product, 4.72 g, 80% yield. ^1H NMR (400 MHz, $CDCl_3$) δ 0.87 (3H, t, *J* = 6.4 Hz), 1.26 – 1.30 (10H, m), 1.60 – 1.64 (2H, m), 3.58 (2H, t, *J* = 7.6 Hz); ^{13}C NMR (100 MHz, $CDCl_3$) δ 14.1, 22.6, 26.8, 28.2, 29.1, 31.7, 38.7, 112.7, 134.8, 160.1; HRMS calcd for $C_{14}H_{17}Br_2NO_2S$ 420.9347, found 420.9338.

5-Octyl-1,3-di(thiophen-2-yl)-4H-thieno[3,4-c]pyrrole-4,6(5H)-dione (11). To a solution of 4.5 g (10.635 mmol) 1,3-dibromo-5-octyl-4H-thieno[3,4-c]pyrrole-4,6(5H)-dione (**10**) in toluene, 2-(tributylstannyl)thiophene (10.317 g, 8.78 mL, 27.652 mmol), tris(dibenzylideneacetone)dipalladium(0) (146.5 mg, 0.16 mmol, 1.5 mol%) and tri(O-tolyl)phosphine (194.1 mg, 0.638 mmol, 6 mol%) were added under nitrogen atmosphere. The reaction mixture was reflux for 18h. After completion of the reaction, the mixture was extracted with dichloromethane. The organic layer was dried over anhydrous magnesium sulfate followed by concentrated under reduced pressure. The crude product was purified by silica gel (230-400 mesh size) column chromatography using hexane-dichloromethane as eluent to afford the yellow powdered product, 3.29 g, 72% yield. ^1H NMR (400 MHz, $CDCl_3$) δ 0.86 (3H, t, *J* = 6.8 Hz), 1.26 – 1.34 (10H, m), 1.63 – 1.71 (2H, m), 3.66 (2H, t, *J* = 7.2 Hz), 7.12 – 7.14 (2H, m), 7.44 (2H, d, *J* = 5.2 Hz), 8.01 (2H, d, *J* = 3.6 Hz); ^{13}C NMR (100 MHz, $CDCl_3$) δ 14.2, 22.7, 27.1, 28.6, 29.3, 31.9, 38.7, 128.5, 128.7, 130.0, 132.5, 136.6, 162.7; HRMS calcd for $C_{22}H_{23}NO_2S_3$ 429.0891, found 429.0885.

1,3-Bis(5-bromothiophen-2-yl)-5-octyl-4H-thieno[3,4-c]pyrrole-4,6(5H)-dione (12). To a solution of 3.2 g (7.448 mmol) 5-octyl-1,3-di(thiophen-2-yl)-4H-thieno[3,4-c]pyrrole-4,6(5H)-dione (**11**) in 1:1 mixture of CH_3COOH – $CHCl_3$ under ice bath, 3.314 g (18.62 mmol) *N*-bromosuccinimide was added in eight portions. The reaction mixture was allowed to come at RT and stirred for 30h. The solvent was evaporated and the residue was purified by silica gel (230-400 mesh size) column chromatography using hexane-dichloromethane as eluent to afford the yellow powdered product, 3.5 g, 80% yield. ^1H NMR (400 MHz, $CDCl_3$) δ 0.86 (3H, t, *J* = 7.2 Hz), 1.26 – 1.31 (10H, m), 1.62 – 1.67 (2H, m), 3.61 (2H, t, *J* = 7.2 Hz), 7.05 (2H, d, *J* = 4.0 Hz), 7.63 (2H, d, *J* = 4.0 Hz); ^{13}C NMR (100 MHz, $CDCl_3$) δ 14.2, 22.8, 27.1, 28.6, 29.3, 31.9, 38.8, 116.9, 128.7, 129.9, 131.3, 133.9, 135.2, 162.4; HRMS calcd for $C_{22}H_{21}Br_2NO_2S_3$ 584.9101, found 584.9113.

General procedure for the Sonogashira coupling: To a solution of aryl halide **12** (1,3-bis(5-bromothiophen-2-yl)-5-octyl-4H-thieno[3,4-c]pyrrole-4,6(5H)-dione) in 1:1 DMF–Et_3N under nitrogen atmosphere, $Pd(PPh_3)_4$ (6 mol%), CuI (3 mol%) and terminal alkyne (**13** – **15**, 2.6 eqv) were added. The reaction mixture was stirred for 24 h at 80 °C and monitored by TLC. After the completion of the reaction, the solvent was evaporated and the resulting residue was purified by silica gel (230-400 mesh size) column chromatography using Hexane-Dichloromethane as eluent to afford the product. The products were isolated with very good yield and characterized by NMR, and mass spectrometry.

View Article Online
DOI: 10.1039/C5RA13416A

General procedure for the Suzuki coupling: To a solution of aryl halide **12** (1,3-bis(5-bromothiophen-2-yl)-5-octyl-4H-thieno[3,4-c]pyrrole-4,6(5H)-dione) in DMF under nitrogen atmosphere, $PdCl_2(PPh_3)_2$ (6 mol%), arylboronic acid (**16** – **17**, 2.5 eqv) and potassium phosphate (K_3PO_4, 6 eqv) were added. The reaction mixture was stirred for 24 h at 80 °C and monitored by TLC. After the completion of the reaction, the solvent was evaporated and the residue was washed with water and extracted by dichloromethane. The crude product was purified by silica gel (230-400 mesh size) column chromatography using Hexane-Dichloromethane as eluent. The products were isolated with very good yield and characterized by NMR, and mass spectrometry.

1,3-bis(5-(phenylethynyl)thiophen-2-yl)- 5-octyl-4H-thieno[3,4-c]pyrrole-4,6(5H)-dione (1). Using the general procedure, to a solution of aryl halide 12 (100.0 mg, 0.170 mmol) in 1:1 DMF–Et_3N under nitrogen atmosphere, $Pd(PPh_3)_4$ (11.8 mg, 0.01 mmol, 6 mol%), CuI (1.0 mg, 0.005 mmol, 3 mol%) and phenylacetylene, 13 (45.0 mg, 0.442 mmol) were added. The title compound 1 was isolated as red solid, 86.7 mg, 81% yield. ^1H NMR (400 MHz, $CDCl_3$) δ 0.88 (3H, t, J = 6.9 Hz), 1.27 – 1.33 (10 H, m), 1.66 – 1.68 (2H, m), 3.63 (2H, t, J = 7.5 Hz), 7.18 (2H, d, J = 3.9 Hz), 7.34 – 7.36 (6H, m), 7.48 – 7.51 (4H, m), 7.84 (2H, d, J = 3.9 Hz); ^{13}C NMR (100 MHz, $CDCl_3$) δ 14.2, 22.8, 27.1, 28.6, 29.3, 31.9, 38.8, 82.4, 96.5, 122.5, 126.7, 128.6, 128.9, 129.1, 129.9, 131.6, 132.9, 133.4, 135.6, 162.4; HRMS calcd for $[C_{38}H_{31}NO_2S_3 + H]^+$ 630.1595, found 630.1571.

1,3-bis(5-((4-methoxyphenyl)ethynyl)thiophen-2-yl)-5-octyl-4H-thieno[3,4-c]pyrrole-4,6(5H)-dione (2). Using the general procedure, to a solution of aryl halide 12 (100 mg, 0.170 mmol) in 1:1 DMF–Et_3N under nitrogen atmosphere, $Pd(PPh_3)_4$ (11.8 mg, 0.01 mmol, 6 mol%), CuI (1.0 mg, 0.005 mmol, 3 mol%) and 4-ethynylanisole 14 (58.4 mg, 0.442 mmol) were added. The title compound 2 was isolated as red solid, 91.5 mg, 78% yield. ^1H NMR (400 MHz, $CDCl_3$) δ 0.85 (3H, t, J = 6.6 Hz), 1.23 – 1.30 (10H, m), 1.64 – 1.66 (2H, m), 3.63 (2H, t, J = 7.2 Hz), 3.81 (6H, s), 6.86 (4H, d, J = 9.0), 7.17 (2H, d, J = 3.9), 7.43 (4H, d, J = 8.7 Hz), 7.86 (2H, d, J = 3.9 Hz); ^{13}C NMR (100 MHz, $CDCl_3$) δ 14.2, 22.8, 27.1, 28.6, 29.3, 31.9, 38.8, 55.5, 81.2, 96.7, 114.3, 127.3, 128.1, 129.0, 130.0, 132.5, 133.0, 133.2, 135.8, 160.2, 162.6; HRMS calcd for $[C_{40}H_{35}NO_4S_3 + H]^+$ 690.1806, found 690.1821.

1,3-bis(5-((4-(dimethylamino)phenyl)ethynyl)thiophen-2-yl)-5-octyl-4H-thieno[3,4-c]pyrrole-4,6(5H)-dione (3). Using the general procedure, to a solution of aryl halide 12 (500 mg, 0.851 mmol) in 1:1 DMF–Et_3N under nitrogen atmosphere, $Pd(PPh_3)_4$ (59.0 mg, 0.051 mmol, 6 mol%), CuI (9.0 mg, 0.026 mmol, 3 mol%) and 4-ethynyl-N,N-dimethylaniline 15 (320.8 mg, 2.212 mmol) were added. The title compound 3 was isolated as red solid, 438.7 mg, 72% yield. ^1H NMR (400 MHz, $CDCl_3$) δ 0.87 (3H, t, J = 6.6 Hz), 1.26 – 1.32 (10H, m), 1.66 – 1.68 (2H, m), 3.00 (12H, s), 3.66 (2H, t, J = 7.2 Hz), 6.66 (4H, d, J = 9.0 Hz), 7.16 (2H, d, J = 4.2 Hz), 7.39 (4H, d, J = 9.0 Hz), 7.89 (2H, d, J = 3.9 Hz); ^{13}C NMR (100 MHz, $CDCl_3$) δ 14.2, 22.8, 27.1, 28.6, 29.3, 31.9, 38.8, 40.3, 81.0, 98.4, 109.0, 110.7, 111.9, 128.1, 128.7, 130.0, 131.8, 132.4, 132.9, 135.9, 150.5, 162.7; HRMS calcd for $C_{42}H_{41}N_3O_2S_3$ 715.2361, found 715.2350.

1,3-bis(5-(4-(dimethylamino)phenyl)thiophen-2-yl)-5-octyl-4H-thieno[3,4-c]pyrrole-4,6(5H)-dione (4). Using the general procedure, to a solution of aryl halide 12 (100 mg, 0.170 mmol) in DMF under nitrogen atmosphere, $PdCl_2(PPh_3)_2$ (7.2 mg, 0.01 mmol, 6 mol%), 4-(N,N-dimethylamino)phenylboronic acid 16 (70.1 mg, 0.425 mmol) and K_3PO_4 (216.2 mg, 1.02 mmol) were added. The title compound 4 was isolated as red solid, 70.1 mg, 61 % yield. ^1H NMR (400 MHz, $CDCl_3$) δ 0.89 (3H, t, J = 6.6 Hz), 1.24 – 1.30 (10H, m), 1.66 – 171 (2H, m), 3.03 (12H, s), 3.68 (2H, t, J = 7.2 Hz), 6.73 (4H, d, J = 9.0 Hz), 7.18 (2H, d, J = 3.9 Hz), 7.55 (4H, d, J = 9.0 Hz), 7.98 (2H, d, J = 4.2 Hz); ^{13}C NMR (100 MHz, $CDCl_3$) δ 14.1, 22.5, 27.0, 28.5, 29.1, 29.6, 31.7, 38.6, 39.7, 111.2, 112.2, 121.9, 125.3, 126.9, 127.4, 128.2, 131.0, 131.4, 134.6, 134.9, 136.6, 152.1, 162.4; HRMS calcd for $C_{38}H_{41}N_3O_2S_3$ 667.2361, found 667.2346.

1,3-bis(5-(4-(diphenylamino)phenyl)thiophen-2-yl)-5-octyl-4H-thieno[3,4-c]pyrrole-4,6(5H)-dione (5). Using the general procedure, to a solution of aryl halide 12 (235 mg, 0.40 mmol) in DMF under nitrogen atmosphere, $PdCl_2(PPh_3)_2$ (16.9 mg, 0.024 mmol, 6 mol%), 4-(N,N-diphenylamino)phenylboronic acid 17 (289 mg, 1.0 mmol) and K_3PO_4 (508 mg, 2.40 mmol) were added. The title compound 5 was isolated as red solid, 242.8 mg, 66 % yield. ^1H NMR (400 MHz, $CDCl_3$) δ 0.90 (3H, t, J = 4.8 Hz), 1.29 – 1.35 (10H, m), 1.68 – 1.70 (2H, m), 3.66 (2H, t, J = 7.3 Hz), 7.05 – 7.16 (16H, m), 7.21 (2H, d, J = 3.9 Hz), 7.28 – 7.33 (8H, m), 7.50 (4H, d, J = 8.7 Hz), 8.00 (2H, d, J = 4.2 Hz); ^{13}C NMR (100 MHz, $CDCl_3$) δ 14.3, 22.8, 27.2, 28.7, 29.4, 31.7, 31.9, 38.7, 123.1, 123.3, 123.6, 125.0, 126.9, 127.1, 128.0, 129.5, 130.8, 131.3, 136.2, 147.3, 147.7, 148.2, 162.7; HRMS calcd for $C_{58}H_{49}N_3O_2S_3$ 915.2987, found 915.2970.

Acknowledgements

The authors are thankful to Pohang University of Science and technology (POSTECH) for support.

References

1. J-Y. Hu, Y-J. Pu, F. Satoh, S. Kawata, H. Katagiri, H. Sasabe, and J. Kido, *Adv. Funct. Mater.*, 2014, **24**, 2064.
2. L. Duan, J. Qiao, Y. Sun, Y. Qiu, *Adv. Mater.*, 2011, **23**, 1137.
3. S. Ren, D. Zeng, H. Zhong, Y. Wang, S. Qian, and Q. Fang, *J. Phys. Chem. B*, 2010, **114**, 10374.
4. S. Ellinger, K. R. Graham, P. Shi, R. T. Farley, T. T. Steckler, R. N. Brookins, P. Taranekar, J. Mei, L. A. Padilha, T. R. Ensley, H. Hu, S. Webster, D. J. Hagan, E. W. V. Stryland, K. S. Schanze, and J. R. Reynolds, *Chem. Mater.*, 2011, **23**, 3805.
5. L. Chen, Y. Jiang, H. Nie, R. Hu, H. S. Kwok, F. Huang, A. Qin, Z. Zhao, and B. Z. Tang, *ACS Appl. Mater. Interfaces*, 2014, **6**, 17215.
6. Z. Cai, Y. Guo, S. Yang,; Q. Peng, H. Luo, Z. Liu, G. Zhang, Y. Liu, and D. Zhang, *Chem. Mater.*, 2013, **25**, 471.
7. S. S. Dharmapurikar, A. Arulkashmir, C. Das, P. Muddellu, and K. Krishnamoorthy, *ACS Appl. Mater. Interfaces*, 2013, **5**, 7086.

8. S. Xu, N. Ai, J. heng, N. Zhao, Z. Lan, L. Wen, X. Wang, J. Peic, and X. Wan, *RSC Adv*., 2015, **5**, 8340.
9. Y. Li, G. Zhang, Z. Liu, X. Chen, J. Wang, C. Di, and D. Zhang, *Macromolecules*, 2013, **46**, 5504.
10. Z. Cai, H. Luo, X. Chen, G. Zhang, Z. Liu and D. Zhang, *Chem.–Asian J.*, 2014, **9**, 1068.
11. T. Lei, Y. Cao, Y. Fan, C-J. Liu, S-C. Yuan, and J. Pei, *J. Am. Chem. Soc*., 2011, **133**, 6099.
12. A. Facchetti, *Chem. Mater*., 2011, **23**, 733.
13. W. Wu, Y. Liu and D. Zhua, *Chem. Soc. Rev*., 2010, **39**, 1489.
14. S. Steinberger, A. Mishra, E. Reinold, C. M. Muller, C. Uhrich, M. Pfeiffer, and P. Bauerle, *Org. Lett*., 2011, **13**, 90.
15. X. Ren, S. Jiang, M. Cha, G. Zhou, and Z-S. Wang, *Chem. Mater*., 2012, **24**, 3493.
16. M. Wang, X. Hu, P. Liu, W. Li, X. Gong, F. Huang, and Y. Cao, *J. Am. Chem. Soc*., 2011, **133**, 9638.
17. K. Takimiya, I. Osaka, and M. Nakano, *Chem. Mater*., 2014, **26**, 587.
18. X. He, B. Cao, T. C. Hauger, M. Kang, S. Gusarov, E. J. Luber, and J. M. Buriak, *ACS Appl. Mater. Interfaces*, 2015, **7**, 8188.
19. E. Castro, A. Cabrera-Espinoza, E. Deemer and L. Echegoyen1, *Eur. J. Org. Chem*., DOI: 10.1002/ejoc.201500552
20. S. Loser, C. J. Bruns, H. Miyauchi, R. P. Ortiz, A. Facchetti, S. I. Stupp, and T. J. Marks, *J. Am. Chem. Soc*., 2011, **133**, 8142.
21. B. He, A. B. Pun, D. Zherebetskyy, Y. Liu, F. Liu, L. M. Klivansky, A. M. McGough, B. A. Zhang, K. Lo, T. P. Russell, L. Wang, and Y. Liu, *J. Am. Chem. Soc*., 2014, **136**, 15093.
22. X. Liu, Y. Sun, B. B. Y. Hsu, A. Lorbach, L. Qi, A. J. Heeger, and G. C. Bazan, *J. Am. Chem. Soc*., 2014, **136**, 5697.
23. F. Huang, K-S. Chen, H-L. Yip, S. K. Hau, O. Acton, Y. Zhang, J. Luo and A. K-Y. Jen, *J. Am. Chem. Soc*., 2009, **131**, 13886.
24. P. Shen, H. Bin, L. Xiao, and Y. Li, *Macromolecules*, 2013, **46**, 9575.
25. K. Li, Z. Li, K. Feng, X. Xu , L. Wang, and Q. Peng, *J. Am. Chem. Soc*., 2013, **135**, 13549.
26. B. Kan, Q. Zhang, M. Li, X. Wan, W. Ni, G. Long, Y. Wang, X. Yang, H. Feng, and Y. Chen, *J. Am. Chem. Soc*., 2014, **136**, 15529.
27. H-H. Chang, C-E. Tsa, Y-Y. Lai, D-Y. Chiou, S-L. Hsu, C-S. Hsu, and Y-J. Cheng, *Macromolecules*, 2012, **45**, 9282.
28. H-I. Lu, C-W. Lu, Y-C. Lee, H-W. Lin, L-Y. Lin, F. Lin, J-H. Chang, C-I. Wu, and K-T. Wong, *Chem. Mater*., 2014, **26**, 4361.
29. A. Mishra, M. K. Fischer and P. Bauerle, *Angew. Chem. Int. Ed.*, 2009, **48**, 2474.
30. C. Teng, X. Yang, C. Yang, H. Tian, S. Li, X. Wang, A. Hagfeldt, and L. Sun, *J. Phys. Chem. C* 2010, **114**, 11305.
31. M. Kivala and F. Diederich, *Acc. Chem. Res*., 2009, **42**, 235.
32. B. Witulski, T. Schweikert, D. Schollmeyer and N. A. Nemkovich, *Chem. Commun*., 2010, **46**, 2953.
33. R. Fitzner, E. Mena-Osteritz, A. Mishra, G. Schulz, E. Reinold, M. Weil, C. Korner, H. Ziehlke, C. Elschner, K. Leo, M. Riede, M. Pfeiffer, C. Uhrich and P. Bauerle, *J. Am. Chem. Soc.*, 2012, **134**, 11064.
34. D. Gajalakshmi, R.V. Solomon, V. Tamilmani, M. Boobalan and P. Venuvanalingam, *RSC Adv*., 2015, **5**, 50353.
35. B. Kan, M. Li, Q. Zhang, F. Liu, X. Wan, Y. Wang, W. Ni, G. Long, X. Yang, H. Feng, Y. Zuo, M. Zhang, F. Huang, Y. Cao, T. P. Russell, and Y. Chen, *J. Am. Chem. Soc.*, 2015, **137**, 3886.
36. J. L. Bredas, R. R. Chance, R. H. Baughman, R. J. Silbey, *Chem. Phys*. 1982, **76**, 3673.
37. J. K.Young, J. S. Moore, Modern Acetylene Chemistry; P. J. Stang, F. Diederich, Eds.; VCH: Weinheim, Germany, 1995, 415-442.
38. M. B. Nielsen, F. Diederich, *Chem. Rev*., 2005, **105**, 1837.
39. U. H. F. Bunz, *Chem. Rev*., 2000, **100**, 1605.
40. R. Chinchilla and C. Najera, *Chem. Rev*., 2007, **107**, 874.
41. R. Chinchilla and C. Najera, *Chem. Soc. Rev*., 2011, **40**, 5084.
42. A. Hilger, J.-P. Gisselbrecht, R. R. Tykwinski, C. Boudon, M. Schreiber, R. E. Martin, H. P. Luethi, M. Gross, F. Diederich, *J. Am. Chem. Soc.* 1997, **119**, 2069.
43. C. R. Swartz, S. R. Parkin, J. E. Bullock, J. E. Anthony, A. C. Mayer, G. G. Malliaras, *Org. Lett.* 2005, **7**, 3163.
44. S. Miao, M. D. Smith, U. H. F. Bunz, *Org. Lett.* 2006, **8**, 757.
45. A. L. Appleton, S. Miao, S. M. Brombosz, N. J. Berger, S. Barlow, S. R. Marder, B. M. Lawrence, K. I. Hardcastle, U. H. F. Bunz, *Org. Lett.* 2009, **11**, 5222.
46. J. E. Anthony, A. Facchetti, M. Heeney, S. R. Marder, X. Zhan, *Adv. Mater.* 2010, **22**, 3876.
47. B. D. Rose, D. T. Chase, C. D. Weber, L. N. Zakharov, M. C. Lonergan, M. M. Haley, *Org. Lett.* 2011, **13**, 2106.
48. W. C. W. Leu, A. E. Fritz, K. M. Digianantonio, and C. S. Hartley, *J. Org. Chem*., 2012, **77**, 2285.
49. W. C. W. Leu and C. S. Hartley, *Org. Lett*., 2013, **15**, 3762.
50. M. A. Saeed, H. T. M. Le, and O. S. Miljanic, *Acc. Chem. Res.*, 2014, **47**, 2074.
51. K. Gao, L. Li, T. Lai, L. Xiao, Y. Huang, F. Huang, J. Peng, Y. Cao, F. Liu, T. P. Russell, R. A. J. Janssen, and X. Peng, *J. Am. Chem. Soc*., 2015, **137**, 7282.
52. G. Jayamurugan, O. Dumele, J-P. Gisselbrecht, C. Boudon, W. B. Schweizer, B. Bernet, and F. Diederich, *J. Am. Chem. Soc.*, 2013, **135**, 3599.
53. B. Liu, W. Zhu, Y. Wang, W. Wu, X. Li, B. Chen, Y-T. Long and Y. Xie, *J. Mater. Chem*., 2012, **22**, 7434.
54. I. Kaur, W. Jia, R. P. Kopreski, S. Selvarasah, M. R. Dokmeci, C. Pramanik, N. E. McGruer and G. P. Miller, *J. Am. Chem. Soc.*, 2008, **130**, 16274.
55. O. L. Griffith, J. E. Anthony, A. G. Jones, Y. Shu, and D L. Lichtenberger, *J. Am. Chem. Soc.*, 2012, **134**, 14185.
56. Y. Wu and W. Zhu, *Chem. Soc. Rev*., 2013, **42**, 2039.
57. B. C. Tlach, A. L. Tomlinson, A. Bhuwalka, and M. Jeffries-EL, *J. Org. Chem.*, 2011, **76**, 8670.
58. Z. Yao, M. Zhang, H. Wu, L. Yang, R. Li, and P. Wang, *J. Am. Chem. Soc*., 2015, **137**, 3799.
59. L. Zophel, V. Enkelmann, and K. Mullen, *Org. Lett.*, 2013, **15**, 804.
60. V. Bhalla, G. Singh, M. Kumar, C. Singh, M. Rawat, and R. S. Anand, *RSC Adv*., 2013, **3**, 14722.
61. A. L. Korich, I. A. McBee, J. C. Bennion, J. I. Gifford, and T. S. Hughes, *J. Org. Chem*., 2014, **79**, 1594.
62. A. Najari, S. Beaupre, P. Berrouard, Y. Zou, J-R. Pouliot, C. Lepage-Perusse, and M. Leclerc, *Adv. Funct. Mater*., 2011, **21**, 718.
63. P. Berrouard, A. Najari, A. Pron, D. Gendron, P-O. Morin, J-R. Pouliot, J. Veilleux, and M. Leclerc, *Angew. Chem. Int. Ed*., 2012, **51**, 2068.
64. A. Najari, P. Berrouard, C. Ottone, M. Boivin, Y. Zou, D. Gendron, W-O. Caron, P. Legros, C. N. Allen, S. Sadki, and M. Leclerc, *Macromolecules*, 2012, **45**, 1833.
65. H. Zhong, Z. Li, F. Deledalle, E. C. Fregoso, M. Shahid, Z. Fei, C. R. Nielsen, N. Yaacobi-Gross, S. Rossbauer, T. D. Anthopoulos, J. R. Durrant, and M. Heeney, *J. Am. Chem. Soc*., 2013, **135**, 2040.

View Article Online
DOI: 10.1039/C5RA13416A

66. J. Yuan, Z. Zhai, H. Dong, J. Li, Z. Jiang, Y. Li, and W. Ma, *Adv. Funct. Mater*., 2013, **23**, 885.
67. Q. Wu, M. Wang, X. Qiao, Y. Xiong, Y. Huang, X. Gao, and H. Li, *Macromolecules*, 2013, **46**, 3887.
68. Y. Zou, A. Najari, P. Berrouard, S. Beaupre, B. R. Aich, Y. Tao, and M. Leclerc, *J. Am. Chem. Soc.*, 2010, **132**, 5330.
69. T-Y. Chu, J. Lu, S. Beaupre, Y. Zhang, J-R. Pouliot, S. Wakim, J. Zhou, M. Leclerc, Z. Li, J. Ding, and Y. Tao, *J. Am. Chem. Soc.*, 2011, **133**, 4250.
70. C. Cabanetos, A. E. Labban, J. A. Bartelt, J. D. Douglas, W. R. Mateker, J. M. J. Frechet, M. D. McGehee, and P. M. Beaujuge, *J. Am. Chem. Soc.*, 2013, **135**, 4656.
71. G-Y. Chen, Y-H. Cheng, Y-J. Chou, M-S. Su, C-M. Chen, and K-H. Wei, *Chem. Commun.*, 2011, **47**, 5064.
72. Q. Feng, X. Lu, G. Zhou, and Z-S. Wang, *Phys. Chem. Chem. Phys.*, 2012, **14**, 7993.
73. Q. Zhang, H. Kuwabara, W. J. Potscavage, Jr., S. Huang, Y. Hatae, T. Shibata, and C. Adachi, *J. Am. Chem. Soc*., 2014, **136**, 18070.
74. Z. R. Grabowksi, K. Rotkiewicz, W. Rettig, *Chem. Rev*., 2003, **103**, 3899.
75. G. M. Badger, I. S. Walker, *J. Chem. Soc.*, 1956, 122.
76. M. J. Frisch et al. Gaussian 03, revision C.02; Gaussian, Inc.: Wallingford, CT, 2004.